

The Updated Bottom Up Solution Applied to Atmospheric Pressure Photoionization and Electrospray Ionization Mass Spectrometry

William Craig Byrdwell¹

Received: 8 July 2015 / Revised: 25 September 2015 / Accepted: 5 October 2015 / Published online: 28 October 2015
© AOCS (outside the USA) 2015

Abstract The Updated Bottom Up Solution (UBUS) was recently applied to atmospheric pressure chemical ionization (APCI) mass spectrometry (MS) of triacylglycerols (TAG). This report demonstrates that the UBUS applies equally well to atmospheric pressure photoionization (APPI) MS and to electrospray ionization (ESI) MS. Critical Ratio 1 (CR1), the $[MH]^+/\Sigma[DAG]^+$ or $[MNH_4]^+/\Sigma[DAG]^+$ ratio, does not exhibit the same strongly sigmoidal shape as it does by APCI-MS. CR1 varies more widely for APPI-MS than by APCI-MS, having a maximum value of 11.8, indicating a much greater effect of unsaturation on ion ratios in APPI-MS than APCI-MS. Critical Ratio 2, the $[AA]^+/[AB]^+$ ratio for Type II TAG or $[AC]^+/([AB]^+ + [BC]^+)$ ratio for Type III TAG, allows quantification of regioisomers of TAG, and shows good agreement for APPI-MS to regioisomer quantification determined by APCI-MS. Critical Ratio 3, the $[BC]^+/[AB]^+$ ratio for Type III TAG, reveals new trends relating the degree of unsaturation by APPI-MS, and shows that structural assignments made by ESI-MS are in good agreement to APCI-MS data. In addition to providing valuable structural information, the Critical Ratios also constitute a reduced data set that allows APPI-MS or ESI-MS mass spectra to be reconstructed when processed through the UBUS. Quantification

by APPI-MS of vitamin D in the gencaps gave values of $42.90 \pm 0.83 \mu\text{g}$, or 1716 ± 33 international units, in good agreement with APCI-MS.

Keywords APPI-MS · ESI-MS · Triacylglycerols · Regioisomers · Lipidomics

Introduction

Human metabolism of triacylglycerols (TAG) is regiospecific, meaning that fatty acids are preferentially metabolized from specific locations on the three carbon atoms of the glycerol backbone, designated by the stereospecific numbering system (*sn*) as *sn*-1, *sn*-2, and *sn*-3. Fatty acids (FA), or more precisely fatty acyl chains, from the outer positions, *sn*-1 and *sn*-3 are preferentially removed from TAG, leaving 2-monoacylglycerols (MAG). TAG synthesis (catabolism) in plants and other animals similarly displays regiospecific trends. In cocoa butter and vegetable oils (VO), the monounsaturated FA (MUFA) oleic acid, 18:1, and the polyunsaturated FA (PUFA) linoleic acid, 18:2, are mainly esterified at the *sn*-2 position [1–3], while saturated FA (SFA) occur preferentially at either the *sn*-1 position [2] or at the *sn*-1 and *sn*-3 positions [1, 3]. Conversely, in fats of animal origin, specifically bovine milk and pork fat (lard), SFA are esterified mainly at the *sn*-2 position, although in beef fat (tallow), SFA are esterified predominantly at the *sn*-1 and *sn*-3 positions [1]. The stereospecific forms of isobaric TAG are regioisomers. The metabolism and catabolism of TAG regioisomers has direct implications for the structures of lipids into which FA are incorporated throughout the human body.

Regioisomerism of TAG is one trait of interest in full structural characterization of TAG. Other, even more

Electronic supplementary material The online version of this article (doi:10.1007/s11746-015-2735-z) contains supplementary material, which is available to authorized users.

✉ William Craig Byrdwell
C.Byrdwell@ars.usda.gov

¹ Food Composition and Methods Development Lab, Beltsville Human Nutrition Research Center, U.S.D.A., Agricultural Research Service, 10300 Baltimore Ave., Beltsville, MD 20705, USA

important, traits include the carbon chain length and degree of unsaturation of the FA. The identities of FA as SFA, MUFA, or PUFA confer much of their influence on health outcomes, such as cholesterol levels, cardiovascular disease and others. For instance, in a 2014 meta-analysis of cohort studies by Schwab *et al.* [4] the findings included: “All of these nine studies found that fasting plasma/serum cholesterol concentration was lower after a diet rich in MUFA and/or PUFA compared with a diet rich in SFA. The evidence was, therefore, considered as convincing.” On the other hand, the now-famous 2014 meta-analysis by Chowdhury *et al.* [5] included the statement: “Current evidence does not clearly support cardiovascular guidelines that encourage high consumption of polyunsaturated fatty acids and low consumption of total saturated fats.” But that report has stirred controversy due to its omission of several important studies and the publication of a correction to some of its findings [6]. Still, there are numerous reports on each side of the controversy.

Regardless of the specifics of any particular association between fats or oils and health outcomes, it is important to have reliable tools for assessing the composition of lipids, especially TAG, in the foods we eat and in biological samples. Toward that end, we have recently published the report of a new tool for structural analysis of TAG, known as the Updated Bottom Up Solution (UBUS) [7]. This was an update of the original Bottom Up Solution (BUS) to the triacylglycerol lipidome using atmospheric pressure chemical ionization mass spectrometry (APCI-MS) [8]. The UBUS (and BUS) employ three Critical Ratios that provide information about different aspects of TAG structure. The first Critical Ratio, $[MH]^+/\Sigma[DAG]^+$, is the ratio of the protonated molecule, $[MH]^+$, over the sum of the diacylglycerol-like fragment ions, $[DAG]^+$. The UBUS showed a new sigmoid function that modeled the average value of Critical Ratio 1 (CR1) *versus* the degree of unsaturation in the TAG.

The second Critical Ratio, $[AA]^+/[AB]^+$ for Type II TAG (ABA, AAB, BAA) and $[AC]^+/([AB]^+ + [BC]^+)$ for Type III TAG (ABC, CBA, BCA, ACB, CAB, BAC), was used to identify and semi-quantify the regioisomers of TAG in soybean oil (SBO), based on published tabulated data of Holcapek *et al.* [9]. The relationship of Critical Ratio 2 (CR2) to the quantification of regioisomers in the UBUS and BUS was based on the foundational work of Jakab *et al.* [10], who showed the use of a calibration curve with the $[AA]^+/[AB]^+$ ratio to quantify the percentage of ABA in mixtures of LOL and LLO regioisomers. That work was simplified by Byrdwell [11] to quantify regioisomers based only on two pure regioisomeric standards, which was demonstrated in the report of the UBUS [7]. The use of Critical Ratio 2 to identify the $[1,3-AC]^+$ regioisomers for Type III TAG was based on the original report of Mottram and

Evershed [12], who showed that the $[1,3-AC]^+ [DAG]^+$ was the smallest of the three $[DAG]^+$ formed by Type III TAG, similar to the work of Laakso and Voutilainen [13], who showed that the $[1,3-AA]^+$ fragment was energetically disfavored for Type II TAG. The correlation of the smallest fragment from Type III TAG with the $[1,3-AC]^+$ fragment held true without exception when the tabulated abundances of Holcapek *et al.* [9] were converted to Critical Ratios 2 and 3, and was used to identify the regioisomers of SBO TAG in the UBUS by APCI-MS.

Byrdwell and Emken reported the first use of HPLC/APCI-MS for TAG in 1995 [14]. In the intervening 20 years, no trends were reported for characterization of the $[1,2-AB]^+$ and $[2,3-BC]^+$ fragments by APCI-MS, and it has always been reported that $[1,2-AB]^+$ and $[2,3-BC]^+$ cannot be distinguished by this technique. Absent such trends, Byrdwell proposed [8] constructing Critical Ratio 3 (CR3), the $[BC]^+/[AB]^+$ ratio, such that $CR3 \leq 1$, where $[BC]^+ \leq [AB]^+$, in the hope that trends would become apparent. Holcapek *et al.* [9] used a different convention, in which $[AB]^+$ and $[BC]^+$ were assigned based on decreasing mass (e.g., OLP instead of PLO), and no trends for $[AB]^+$ *versus* $[BC]^+$ were apparent in their data. However, when the data of Holcapek *et al.* [9] were rearranged and the Critical Ratios were constructed according to the Byrdwell convention [8], trends for 25 of 27 Type III TAG regioisomers were identified [7]. Byrdwell showed [7] that the predominant factor dictating the fragmentation of TAG other than the $[1,3-AC]^+$ fragment is the grouping or separation of unsaturated FA on the glycerol backbone.

Although trends for factors that influenced the relative abundances of $[AB]^+$ *versus* $[BC]^+$ were reported, the approach of Byrdwell [7] did not localize FA to exact *sn*-1 or *sn*-3 positions. In Type II TAG, AAB and BAA are enantiomers that cannot be distinguished by any of the atmospheric pressure ionization (API)-MS techniques, (i.e. APCI-MS, APPI-MS, or ESI-MS). Similarly, in Type III TAG, although the FA in the *sn*-2 position can be identified, ABC cannot be distinguished from its enantiomer CBA. Enantiomers can only be differentiated using chiral chromatography (CC) [15–18]. Even so, not all isomers may be separable using CC, depending on the column and conditions used. In some cases, TAG that contain SFA combined with di-unsaturated (e.g. linoleic acid, L) or tri-unsaturated (e.g. linolenic acid, Ln) FA in the *sn*-1 and *sn*-3 positions were not separated, such as LPP/PPL, LOP/POL, LLP/PLL, AALn/LnAA, LnOA/AOLn and LnLnA/ALnLn [16], while in other cases enantiomers such as LLP/PLL were separated [18]. Still, even when separated using CC, the mass spectra showed negligible or no differences between enantiomers. Therefore, the trends reported by Byrdwell [7] can be expected to apply to both enantiomers in a pair. For simplicity, when referring to $[1,3-AC]^+$

[DAG]⁺ below, such as would arise from loss of the *sn*-2 “B” FA from ABC TAG, it should be realized that this also refers to the CBA enantiomer that gives [3,1-AC]⁺. Similarly, [1,2-AB]⁺ from ABC cannot be distinguished from [2,3-AB]⁺ from the CBA enantiomer, so these are referred to as [1,2(2,3)-AB]⁺ herein.

APPI-MS and ESI-MS produce simple mass spectra of TAG, having mainly [MH]⁺ or [MNH₄]⁺ ions, respectively, and [DAG]⁺ ions, similar to mass spectra obtained by APCI-MS. Therefore, it could be expected that the BUS [8] and UBUS [7] for APCI-MS should apply equally well to the other API-MS techniques. However, this must be proved with certainty, using data such as that acquired using the triple-parallel mass spectrometry (LC1/MS3) approach that we have reported previously, in which all three of these API-MS techniques were employed simultaneously for analysis of the same samples [19]. Toward that end, reported here is the first use of Critical Ratios to characterize TAG structures by APPI-MS, ESI-MS, and MS/MS and comparison to the trends identified by APCI-MS.

Materials and Methods

Acetonitrile, methanol (MeOH), acetone, and dichloromethane (DCM) Optima LC–MS grade were purchased from Thermo Fisher Scientific, Inc. (Hanover Park, IL). Five samples of vitamin D₃ dietary supplement gelcaps (507.25 ± 1.94 mg) containing 2000 international units (IU, where 1 IU = 0.25 μg) in ~500 mg soybean oil were prepared using the “dilute-and-shoot” approach described previously [19]. 2.0 mL of 25 μg/mL vitamin D₂ internal standard (=2000 IU, or 0.50 μg/mL in final solution) was added and samples were diluted to 100 mL in MeOH/DCM (60:40). According to the product label, the vitamin D₃ was “molecularly distilled” from fish oil. Each sample was analyzed in triplicate, for a total of 15 runs.

Separation of TAG was accomplished using non-aqueous reversed-phase (NARP) HPLC using two Inertsil ODS-2 RP columns in series (25 cm × 4.6 mm, 5 μm) on an Agilent 1200 system, for which the gradient program has been described elsewhere [19].

ESI-MS was conducted on an LCQ Deca XP mass spectrometer (ThermoScientific, Inc., San Jose, CA) using the parameters previously described [19] and dopant-assisted APPI-MS was performed on a QTrap 4000 hybrid mass spectrometer (AB Sciex, Inc., Framingham, MA) having a Photospray[®] source (using a krypton UV lamp), with acetone added as dopant via an Agilent Technologies (Santa Clara, CA) 1290 UHPLC at 40 μL/min and other

parameters the same as those used for ESI-MS on that instrument, previously described [19].

The response-factor adjusted TAG percentage compositions were determined as described in the report of the UBUS by APCI-MS. The method of Byrdwell *et al.* [20, 21] was used to apply response factors, in which the FA composition calculated from the raw TAG composition was compared to the FA composition determined by calibrated GC-FID (parameters given in Ref. [22]) to produce FA response factors, which were multiplied together to produce TAG response factors. The spreadsheet to accomplish this quantification has been published elsewhere as electronic supplementary material (ESM) [7] and is available online at <http://www.ars.usda.gov/services/software/software.htm?modecode=80-40-05-05>. The 1 × ¹³C isotope peaks were included to increase signal without loss of specificity [22, 23], extracted ion chromatograms (EICs) for [MH]⁺ and [DAG]⁺ were grouped for each TAG to reduce the number of EICs integrated and increase the signal for the each TAG EIC group [22].

Critical Ratios were calculated from the average mass spectra over the retention time windows of the integrated peaks, obtained by pasting the beginning and ending retention times of the integrated peaks into the XCalibur[™] Qual Browser or Analyst[™] software, and copying the resultant spectra into a spreadsheet. The spreadsheet to allow calculation of the mass spectra from the Critical Ratios has also been made freely available online at <http://www.ars.usda.gov/services/software/software.htm?modecode=80-40-05-05>. Isotope correction was performed on the mass spectra using isotope ratios calculated from ChemCalc.org [24], which is based on the algorithm of Yamamoto and McCloskey [25].

Vitamin D₃ quantification by APPI-MS was performed using EICs from full scans (including the 1 × ¹³C masses for increased signal without loss of specificity) and by selected ion monitoring (SIM) using *m/z* 367.3 and *m/z* 385.3 for vitamin D₃ with *m/z* 379.3 and *m/z* 397.3 for the vitamin D₂ internal standard (IS). Raw areas obtained from peaks in these chromatograms were weight-normalized (avg. weight 507.25 mg per capsule) for equal weight comparison. Our approach to quantification in oil-filled gelcaps has been described elsewhere [19].

The following FA abbreviations are used (carbon chain length: sites of unsaturation): Cy: caprylic acid (C8:0); Ca: capric acid (C10:0); M: myristic acid (C14:0); Po: palmitoleic acid (C16:1); P: palmitic acid (C16:0); Ln: linolenic acid (C18:3); L: linoleic acid (C18:2); O: oleic acid (C18:1); S: stearic acid (C18:0); G: gadoleic acid (C20:1); A: arachidic acid (C20:0); E: erucic acid (22:1); B: behenic acid (22:0); Lg: lignoceric acid (C24:0); Ce: cerotic acid (C26:0); Mo: montanic acid (C28:0).

Table 1 Response-factor-adjusted percentage composition and isotope-adjusted Critical Ratios for soybean oil from vitamin D₃ supplement gel-cap determined by APPI-MS on the Qtrap 4000 mass spectrometer

TAG	RT	% Comp.	[MH] ⁺ /Σ[DAG] ⁺	[AA] ⁺ /[AB] ⁺	Case	
CyCyCy	12.70	24.83	0.0343		1	
CyCyCa	16.57	46.11	0.0317	0.5544	1.1	
CaCaCy	22.15	29.06	0.0341	0.5666	1.1	
TAG	RT (min)	% Comp.	[MH] ⁺ /Σ[DAG] ⁺	[AA] ⁺ /[AB] ⁺ or [AC] ⁺ / ([AB] ⁺ + [BC] ⁺)	[BC] ⁺ /[AB] ⁺	Case
LnLnLn	46.71	0.08	11.8486			2
LnLLn	49.49	1.25	7.8794	0.4197		2.1
LLLn	52.87	5.22	1.9042	0.6676		2.1
<i>LnOLn</i>	53.59	0.64	8.1139	0.4110		2.1
<i>LnLM</i>	54.96	0.09	2.9176	0.1874	0.3993	2.1.1
<i>LnLnP</i>	55.39	0.31	8.5939	0.8052		2.1
LLL	56.98	12.46	1.2804			2
<i>LLnO^a</i>	57.83	3.86	1.4393	0.4057	0.8613	2.1.1
<i>LLM</i>	59.58	0.42	1.5847	2.3409		2.2
LnLP	59.93	3.52	2.1974	0.3315	0.8061	2.1.1
<i>LnPPo</i>	60.54	0.07	1.2466	0.1988	0.4740	2.1.1
<i>LnOM</i> (14)	60.60	0.09	1.4181	0.1235	0.4912	2.1.1
LLO	62.69	12.97	0.8480	0.8985		2.1
<i>OLPo</i>	63.77	0.29	0.4887	0.1541	0.2081	1.1.1
<i>OLnO</i>	63.94	1.52	2.7457	0.3787		2.1
LLP	65.25	11.91	0.8199	0.9350		2.1
<i>LOM</i>	66.23	0.37	0.7812	0.2115	0.4575	2.1.1
<i>PoLP</i>	66.30	0.41	0.3704	0.1407	0.8591	1.1.1
LnOP	66.39	1.40	2.3608	0.3601	0.6104	2.1.1
<i>LLG</i>	67.98	0.72	2.6951	2.5335		2.2
<i>PLM</i>	69.08	0.12	0.1376	0.2603	0.4800	1.1.1
<i>PLnP</i>	69.33	0.30	2.2628	0.3205		2.1
OLO	69.70	7.40	0.8424	0.4977		2.1
<i>MOM</i> (9)	70.35	0.03	0.2114	0.4383		1.1
<i>OOPo</i>	71.41	0.16	0.1308	3.8421		1.2
LLS	71.60	6.92	1.6728	0.9646		2.1
<i>LnLA</i>	71.28	0.13	2.3103	0.1866	0.2695	2.1.1
OLP	72.75	8.97	0.5737	0.3799	0.7267	2.1.1
<i>SLnO</i>	73.09	0.46	0.6805	0.0767	0.1771	1.1.1
<i>OOM</i>	74.08	0.16	0.3080	0.5928		1.1
<i>PPoO^d</i>	74.23	0.16	0.1799	0.4612	0.8503	1.1.1
<i>OLG</i>	75.60	0.45	0.9998	0.1930	0.4211	2.1.1
PLP	76.13	2.31	0.2382	0.3959		1.1
<i>POM</i>	77.89	0.12	0.1455	0.3132	0.8372	1.1.1
OOO	77.84	2.03	0.5635			1
<i>LnLB</i> (14)	78.39	0.14	3.4841	0.2754	0.7321	2.1.1
<i>LLA</i>	78.46	0.49	3.0652	1.3029		2.2
<i>PLG^a</i>	79.09	0.26	1.8820	0.3398	0.6835	2.1.1
OLS	79.92	3.75	0.8088	0.3303	0.6585	2.1.1
OOP	81.53	1.88	0.2925	0.5806		1.1
<i>LL-21:0</i> (9)	81.96	0.08	1.8014	3.0339		2.2
<i>OLE</i>	82.84	0.05	0.8619	0.2327	0.3620	2.1.1
PLS	83.89	1.53	0.2281	0.2730	0.9778	1.1.1
<i>OOG</i>	84.35	0.20	0.3005	1.8295		1.2

Table 1 continued

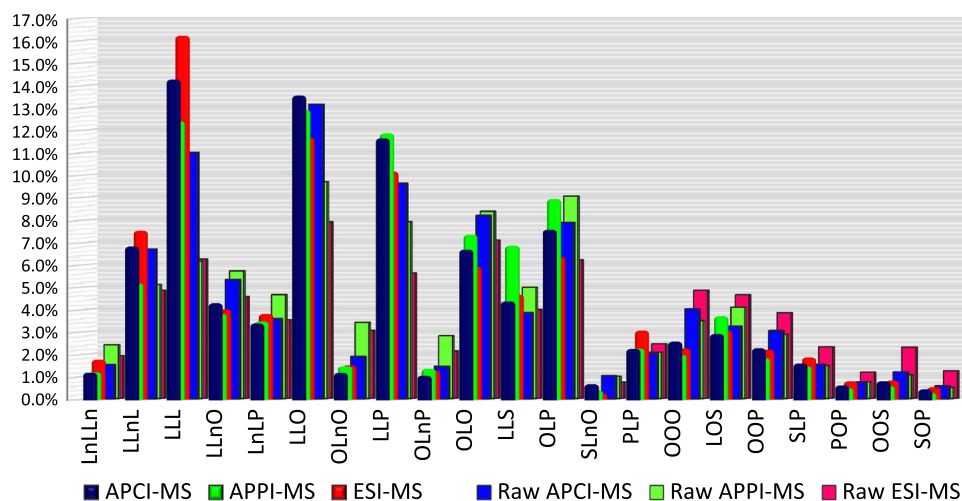
TAG	RT (min)	% Comp.	[MH] ⁺ /Σ[DAG] ⁺	[AA] ⁺ /[AB] ⁺ or [AC] ⁺ / ([AB] ⁺ + [BC] ⁺)	[BC] ⁺ /[AB] ⁺	Case
<i>LnLLg</i> (6)	85.46	0.04	3.5506	0.2470	0.4993	2.1.1
<i>POP</i>	85.70	0.56	0.1917	0.2721		1.1
LLB	85.74	0.52	2.8851	1.1502		2.2
<i>OLA</i>	87.66	0.17	0.9519	0.3124	0.5875	2.1.1
<i>OPG</i>	88.73	0.12	0.3666	0.3276	1.0013	1.1.2
<i>LL-23:0</i>	89.56	0.09	2.3217	2.2245		2.2
OOS	89.68	0.65	0.3195	0.6388		1.1
<i>LO-21:0</i>	91.93	0.04	0.6068	0.1624	0.2333	1.1.1
<i>PPP</i>	91.76	0.01	0.0135			1
<i>A₁PL</i>	92.08	0.16	0.5119	0.3671	0.7175	2.1.1
SLS	92.14	0.32	0.3168	0.3654		1.1
<i>OOE</i>	92.26	0.07	0.1454	3.9729		1.2
LLg	93.33	0.17	2.6847	1.1123		2.2
POS	94.13	0.34	0.1977	0.2006	0.8049	1.1.1
OLB^a	95.53	0.19	0.8255	0.3354	0.6071	2.1.1
OPE	96.77	0.03	0.3780	0.3697	0.8305	1.1.1
<i>GSO</i>	96.87	0.04	0.5634	0.3173	0.7987	2.1.1
<i>LL-25:0</i>	97.21	0.03	1.7139	2.4102		2.2
OOA	97.76	0.04	0.2934	0.7352		1.1
<i>LO-23:0</i>	99.52	0.03	0.6963	0.2370	0.3300	2.1.1
PLB	99.97	0.12	0.2771	0.3248	0.9394	1.1.1
<i>ASL</i>	100.22	0.06	0.4690	0.4176	0.6919	2.1.1
<i>PPS</i>	101.11	0.00	0.0304	0.9232		1.1
<i>LLCe</i>	101.05	0.03	1.7657	1.9462		2.2
<i>OO-21:0</i>	101.98	0.00	0.2453	1.7155		1.2
<i>APO</i>	102.91	0.04	0.4583	0.3640	0.9353	2.1.1
SOS	102.90	0.08	0.2737	0.2965		1.1
<i>OLLg</i>	103.55	0.07	0.6775	0.2968	0.5570	2.1.1
OOB	105.82	0.05	0.2863	0.6084		1.1
<i>OL-25:0^c</i> (14)	107.25	0.01	0.5339	0.2360	0.3370	1.1.1
<i>PLLg</i>	107.75	0.05	0.4077	0.4384	0.8362	2.1.1
BLS	108.22	0.05	0.3319	0.3301	0.9459	1.1.1
<i>OO-23</i>	109.32	0.01	0.2179	1.2296		1.2
POB (14)	109.63	0.03	0.2611	0.2537	0.7784	1.1.1
<i>OLCe</i>	110.35	0.02	0.5773	0.2138	0.4678	2.1.1
<i>ASO</i>	110.40	0.01	0.4791	0.4389	0.8774	2.1.1
OOLg	112.49	0.02	0.2417	0.6338		1.1
SLLg	114.45	0.01	0.2351	0.2637	0.8282	1.1.1
<i>OO-25</i> (11)	115.22	0.00 ^b	0.1859	1.5149		1.2
POLg	115.88	0.01	0.2217	0.2075	0.7579	1.1.1
<i>BOS</i> (3)	110.66	0.00	0.1532	0.0855	1.5589	1.1.2
<i>OOCe</i> (2)	113.75	0.00	0.3551	1.8791		1.2
<i>SLCe</i> (1)	115.95	0.00	0.1738	0.2104	0.4612	1.1.1
<i>LgOS</i> (2)	117.65	0.00	0.1404	0.2731	0.9376	1.1.1
<i>OOMo</i> (2)	118.36	0.00	0.0000	35.9151		1.2
Sum		100.00	Avg. = 1.2815			

TAG name indicates most abundant regioisomer, as indicated by Critical Ratio 2, and order of fatty acyl chains indicated by Critical Ratio 3 set to minimum. Boldface indicates clean spectrum; italics indicate spectrum contains substantial peaks from more than one TAG. Parentheses indicate number of scans averaged, if < 15. Underlining indicates structure assigned different from APCI-MS

^a Order of FA changed after isotope correction

^b Values of 0.00 % were present at less than 0.005 %

Fig. 1 Response-factor-normalized and un-normalized (raw) triacylglycerol (TAG) percentage compositions determined by atmospheric pressure chemical ionization (APCI) mass spectrometry (MS), atmospheric pressure photoionization (APPI) MS and electrospray ionization (ESI) MS. Abbreviations given in “Materials and Methods” section. APCI-MS data from Ref. [7]



Results and Discussion

Table 1 shows the Critical Ratios obtained from the mass spectra of integrated chromatographic peaks from APPI-MS and the percentage composition of TAG. The Case classification in the last column is used to reproduce the exact mass spectrum from the Critical Ratios when processed through the UBUS, but also indicates the overall properties of the mass spectrum at face value. Specifically, for *n.n.n*, if the first “*n*” is 2, the $[MH]^+$ or $[MNH_4]^+$ is the base peak, or if it is 1 a $[DAG]^+$ is the base peak; if the second “*n*” is 1 (as is usual), the $[AA]^+$ (Type II TAG) or $[AC]^+$ (Type III TAG) peak is smaller than $[AB]^+$ and $[BC]^+$, otherwise $[AA]^+$ or $[AC]^+$ is larger; if the third “*n*” (Type III TAG) is 1, $[BC]^+$ is less than $[AB]^+$, otherwise, the inverse is true.

Three short-chain TAG were identified (CyCyCy, CyCyCa, and CaCaCy) that did not originate from the soybean oil, and so were quantified separately from the SBO TAG. These arose from the fact that the vitamin D₃ came from “molecularly distilled” fish oil, which contained these TAG along with vitamin D₃. We previously reported that a different and seemingly unrelated brand of vitamin D₃ supplements that used vitamin D₃ from fish oil contained these same three TAG [19].

The reason that the Critical Ratios are provided to four decimal places is to minimize rounding error when converting to raw abundances in the UBUS. The Critical Ratios can be converted to abundances, and from abundances back to Critical Ratios (to confirm the validity of the model), and back and forth many times using the spreadsheet provided before rounding error affects the results. Figure 1 depicts the TAG compositions for molecular species present in amounts greater than 0.5 % by APCI-MS (in blue), APPI-MS (in green), and ESI-MS

(in red), which shows the percentage compositions before and after application of TAG response factors (RF) for the three API techniques. The three front sets of columns represent the response-factor-normalized compositions, while the three back sets of columns represent the raw, un-normalized compositions. The FA compositions calculated from the RF-normalized and un-normalized TAG compositions for APPI-MS and ESI-MS and from gas chromatography (GC) with flame ionization detection (FID) are given in Table 2. The complete set of FA compositions from normalized and raw TAG compositions for all three API techniques are given in Fig. 2, with the columns in the same order and using the same colors as Fig. 1, but with the GC-FID results added at the front. Results in Fig. 2 show that, especially for the major FA, the un-normalized APCI-MS results were closer to the GC-FID results, and that application of response factors brought APCI-MS, APPI-MS, and ESI-MS results into good agreement with each other and with the GC-FID results. Some trends can be seen in Fig. 1 in the response of the un-normalized TAG to APPI-MS and ESI-MS compared to APCI-MS (back three data series). For instance, several TAG that contained the ‘LL’ diacylglycerol, i.e. LLLn, LLL, LLO, and LLP, gave lower response by both APPI-MS and ESI-MS than by APCI-MS. On the other hand, TAG containing ‘LnL’, i.e. LnLLn, LnLO, and LnLP (but not LnLL, see above), responded more by APPI-MS than by APCI-MS, as did several TAG containing ‘OLn’, i.e. OLnL, OLnO, OLnP. In contrast, several TAG with few sites of unsaturation gave higher un-normalized signal by ESI-MS than APCI-MS and APPI-MS (taller pink bars at right end of Fig. 1). Differences in response between API techniques is a worthy topic for future detailed discussion, but is not the primary objective of this report.

Table 2 Mole percent fatty acid (FA) composition from FA methyl esters by GC with flame ionization detection (FID) and response factor normalized triacylglycerol (TAG) compositions determined by atmospheric pressure photoionization (APPI) mass spectrometry (MS) and electrospray ionization (ESI) MS

FA	GC-FID (%)	APPI-MS (%)	ESI-MS (%)
Cy	64.41	68.77	61.37
Ca	35.59	31.23	38.63
Sum	100.00	100.00	100.00
M	0.48	0.48	0.46
Po	0.51	0.43	0.47
P	12.17	12.61	12.49
Ln	7.62	7.22	8.37
L	50.47	50.83	51.71
O	23.22	21.97	20.54
S	4.11	4.86	4.39
A	0.31	0.37	0.35
G	0.52	0.59	0.56
21	0.03	0.04	0.04
B	0.31	0.36	0.36
E	0.04	0.05	0.06
23	0.03	0.04	0.04
Lg	0.11	0.13	0.13
N	0.03	0.00	0.00
25	0.01	0.02	0.02
Ce	0.01	0.02	0.02
Mo	0.00	0.00	0.00
Sum	100.00	100.00	100.00
%DAG/TAG		0.26	0.06

^a Short-chain TAG were from fish oil (source of vitamin D), not from soybean oil TAG

Critical Ratio 1, $[MH]^+/\Sigma[DAG]^+$

In the first report of the UBUS [7], the sigmoid model for CR1 by APCI-MS was presented, which provided a good estimate of the average values of CR1 *versus* the number of sites of unsaturation in the SBO TAG. The values for CR1 by APPI-MS and ESI-MS were very different from those by APCI-MS, so the sigmoid model does not describe the behavior of those API techniques. For APPI-MS, CR1 had a much wider range than by APCI-MS. As seen in Table 1, the maximum value of CR1 by APPI-MS was 11.85 (*versus* 4.60 by APCI-MS), demonstrating a much larger effect for some TAG due to degree of unsaturation for APPI-MS than APCI-MS. But this was not universally true, since LLL, for instance, gave a ratio of 1.28 by APPI-MS *versus* 2.66 by APCI-MS [7]. At the other end of the range of unsaturation, saturated TAG such as PPS gave similar very low values of CR1, i.e. 0.03 by APPI-MS *versus* 0.002 by APCI-MS, indicating that both techniques produced very little $[MH]^+$ from TAG with few or no sites

of unsaturation. While the much wider range of values for CR1 by APPI-MS compared to APCI-MS cannot yet be fully explained, characterized, or modeled, CR1 provides a new tool to begin the process of such characterization.

ESI-MS gave ammonium adducts, $[MNH_4]^+$, so CR1 by ESI-MS, Table 3, is composed of $[MNH_4]^+/\Sigma[DAG]^+$, exactly analogous to the $[MH]^+/\Sigma[DAG]^+$ used for APCI-MS and APPI-MS. However, ESI-MS generally gave larger values for CR1, as expected from the well-known fact that TAG produce $[MNH_4]^+$ base peaks by ESI-MS. This is reflected in the Case classification given in the last column in Table 3, in which every TAG is Case 2 for CR1, without exception. The ability of ESI-MS to give complementary data in the form of abundant ammonium adducts, even for saturated TAG, is the reason it is included in our triple- and quadruple-parallel mass spectrometry experiments. The average value for the $[MNH_4]^+/\Sigma[DAG]^+$ was 6.2732. Values that were very much larger (~12.0) or smaller (~1.0–2.0) than the average value most often provided indications of overlap of neighboring peaks. Figure 3 illustrates the relationship between CR1 and the percentage of TAG present, with a red line indicating the approximate 0.50 % level. Figure 3 reflects the fact that all TAG present at >0.6 % had values for CR1 between 5.4516 (for PLP, at 3.09 %) and 7.3481 (for OLnO, at 1.54 %). On the other hand, the TAG at lower levels showed disparate values for CR1. For example, the lowest value for CR1 is 1.3736 for OOPo at 71.18 min, and 0.19 %. As Table 3 shows, that peak is next to LLS at 71.63 min, and 4.70 %. These two TAG shared a common ion at m/z 603.5, representing $[OO]^+$ from OOPo and $[SL]^+$ from LLS, but OOPo and LLS have different molecular masses and different $[MH]^+$ ions. Thus, a contribution to the abundance of the $[OO]^+$ ion from the much larger $[SL]^+$ from LLS led to a larger $\Sigma[DAG]^+$ for OOPo, so a lower than expected $[MH]^+/\Sigma[DAG]^+$. On the other hand, PGL at 79.30 min and 0.31 % (Table 3) gave a value for CR1 of 12.5441 because it had the same $[MH]^+$ as the neighboring SLO at 80.04 min, present at 3.10 %. Therefore, the contribution of the $[MH]^+$ from SLO gave a larger contribution to the $[MH]^+/\Sigma[DAG]^+$ than the $[SO]^+$ from SLO that was isobaric with $[PG]^+$ from PGL, resulting in a larger than expected CR1 for PGL.

Thus, when CR1 is lower than expected by ESI-MS, an overlapping $[DAG]^+$ ion from TAG species with different $[MH]^+$ ions can be expected, whereas when CR1 is higher than expected, an overlapping $[MH]^+$ from isobaric TAG is indicated. Thus, CR1 provides a diagnostic tool and a marker for influences of overlapping ions by ESI-MS. From these observations, it is obvious that the mass spectra of pure, isolated TAG standards in the absence of TAG having the same equivalent carbon number ($ECN = \#$ carbons in acyl chains $- 2 \times \#$ double bonds) will be different,

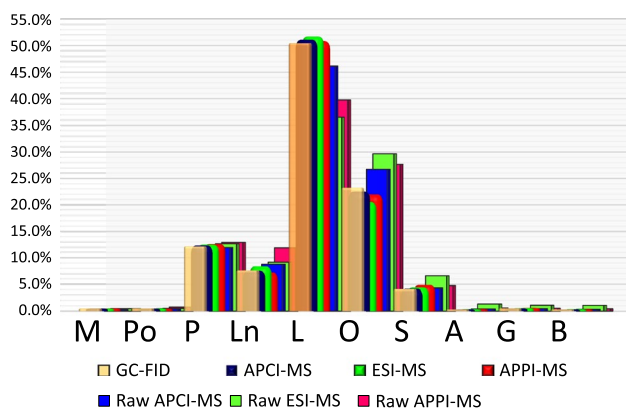


Fig. 2 Fatty acid (FA) compositions from response-factor-normalized and un-normalized (raw) triacylglycerol (TAG) percentage compositions in Fig. 1, plus FA composition determined by gas chromatography (GC) with flame ionization detection (FID) of FA methyl esters

and give different Critical Ratios, than the same TAG in real mixtures containing TAG with the same ECN, and therefore similar retention times by RP-HPLC. While the Critical Ratios will be affected by partial overlap of closely related, not completely resolved TAG, the UBUS reproduces the exact mass spectra observed by all API techniques, whether overlapped or not.

MS/MS mass spectra of the $[M + NH_4]^+$ ions by ESI-MS gave smaller values of CR1, Supplementary Table 1, reflecting the fact that the spectra were more similar to APCI-MS. The average CR1 by ESI-MS/MS was 0.4242, compared to 0.7790 by APCI-MS and 1.2815 by APPI-MS. Examination of the Case classifications in the last column of S-Table 1 showed Case classifications for TAG very similar to those reported by APCI-MS, indicating similar appearance of mass spectra. ESI-MS/MS data were not obtained for every TAG, because the automated MS/MS instrument routine did not identify minor TAG as one of the most abundant ions and perform auto-MS/MS in some cases of overlapped TAG. Because of space limitations, ESI-MS/MS spectra are not discussed in detail here, but data are provided to prove that the UBUS applies equally well to ESI-MS/MS as it does to ESI-MS, APCI-MS, and APPI-MS.

Critical Ratio 2 for Type II TAG

Table 4 shows semi-quantification of TAG regioisomers by APPI-MS, ESI-MS and ESI-MS/MS, compared to the recently reported values for APCI-MS, calculated using Equation 2 from the first report of the UBUS [7]. Quantification was performed using values for CR2 obtained by APCI-MS, since extensive and detailed tabulated data for synthesized regioisomeric standards, such as those

presented by Holcapek *et al.* [9], are not available for APPI-MS and ESI-MS. Only few regioisomeric standards that are commercially available have been analyzed by ESI-MS, and we are not aware of any data for regioisomer standards by APPI-MS. Byrdwell has tabulated APCI-MS and ESI-MS data [8, 11, 26], and repeatedly shown that the $[AA]^+/[AB]^+$ ratios obtained by ESI-MS are similar to those obtained by APCI-MS, so those obtained by APPI-MS should be expected to also be close to those obtained by APCI-MS (especially given the overall similarity between APPI-MS and APCI-MS mass spectra). Note that $[AA]^+/[AB]^+ = [AA]^+ / ([AB]^+ + [BA]^+)$, since $[AB]^+$ cannot be distinguished from $[BA]^+$, as previously mentioned [7, 8].

Table 4 indicates that the specific regioisomers identified by APPI-MS were the same as those identified by APCI-MS in every case except dilinoleoyl, linolenoyl triacylglycerol, LLnL. This reinforces the overall similarity between spectra obtained by APPI-MS and APCI-MS, and is not particularly surprising. The ability to use APCI-MS data for semi-quantification of TAG regioisomers by APPI-MS is tremendously beneficial, since it allows wider use of APCI-MS data, and allows more information to be extracted from APPI-MS data.

Since the results for CR1, above, showed a much larger effect (larger CR1) for APPI-MS due to unsaturation than APCI-MS, it is possible that the reason the LLnL, which was a fairly pure chromatographic peak, was unique and dramatically different from APCI-MS is because ‘Ln’ was a better leaving group, and so its loss from the *sn*-2 position was less energetically disfavored than other FA at that position. This would be further assisted by the stability of the remaining polyunsaturated $[LL]^+$ ion, which is why OLnO and PLnP did not follow the same behavior for Ln at *sn*-2 by APPI-MS. If true, the behavior of LLnL would be similar to the trends reported by Byrdwell that explained the behavior of CR3 for 25 of the 27 TAG regioisomers [7]. Overall, however, there was excellent agreement between the structural assignments made based on APPI-MS and those made by APCI-MS. Nevertheless, quantification would be expected to improve if APPI-MS data for regioisomeric standards were available. Thus, there is a real need for the same kind of data for APPI-MS that Holcapek *et al.* [9] reported for APCI-MS.

The quantification of regioisomers by ESI-MS based on comparison to APCI-MS data was less effective. Four TAG were assigned as different primary regioisomers based on ESI-MS, with several others being near the 50 % cut-off used to assign the primary regioisomer. CR2 does, however, provide insight into the reason for these differences. It is an unlikely coincidence that every TAG that was assigned differently contained an $[LL]^+$ diacylglycerol-like fragment (i.e., LLnL, LLO, LLP, LLB), and almost

Table 3 Response-factor-adjusted percentage composition and isotope-adjusted critical ratios for soybean oil from vitamin D₃ supplement gel-cap determined by ESI-MS on the LCQ Deca XP ion trap mass spectrometer

TAG	RT	% Comp.	[MNH ₄] ⁺ /Σ[DAG] ⁺	[AA] ⁺ /[AB] ⁺	Case	
CyCyCy	12.75	22.98	14.8747		2	
CyCyCa	16.62	45.13	11.7890	0.4518	2.1	
CaCaCy	22.19	31.89	9.9792	0.5490	2.1	
TAG	RT (min)	Comp.	[MNH ₄] ⁺ /Σ[DAG] ⁺	[AA] ⁺ /[AB] ⁺ or [AC] ⁺ /([AB] ⁺ + [BC] ⁺)	[BC] ⁺ /[AB] ⁺	Case
LnLnLn	46.80	0.13	5.6647			2
LnLLn	49.57	1.80	6.1163	0.4825		2.1
LLLn	52.93	7.57	6.2109	0.5329		2.1
<i>LnOLn</i>	53.68	0.59	8.2185	0.3559		2.1
<i>LnLM</i>	55.09	0.10	2.4260	0.1736	0.2509	2.1.1
<i>LnLnP</i>	55.49	0.38	5.9226	0.5896		2.1
LLL	56.94	16.24	6.1926			2
<i>OLnL^a</i>	57.91	4.05	6.1485	0.4201	0.7768	2.1.1
<i>LLM</i>	59.58	0.34	3.4898	1.3731		2.2
LnLP	60.00	3.84	5.8676	0.4540	0.9029	2.1.1
<i>LnPPo</i>	60.69	0.10	1.8680	0.1018	0.2438	2.1.1
<i>LnOM</i>	60.83	0.08	2.7671	0.1210	0.4346	2.1.1
LOL	62.73	11.71	6.2621	0.5708		2.1
<i>OLPo^a</i>	63.84	0.21	2.1598	0.1701	0.2070	2.1.1
<i>OLnO</i>	63.84	1.54	7.3481	0.4116		2.1
LPL	65.27	10.20	5.8178	0.6024		2.1
<i>LOM</i>	66.28	0.33	3.3034	0.1460	0.2651	2.1.1
<i>PoLP</i>	66.35	0.53	1.4014	0.0880	0.5142	2.1.1
OLnP^a	66.57	1.32	6.3173	0.4337	0.7732	2.1.1
<i>LLG</i>	67.98	0.58	5.3970	1.1716		2.2
<i>PLM</i>	69.11	0.07	3.2482	0.2504	0.4842	2.1.1
<i>PLnP</i>	69.31	0.15	5.4899	0.4253		2.1
OLO	69.72	5.96	6.2683	0.4571		2.1
<i>MOM</i>	70.64	0.04	5.9344	0.3434		2.1
<i>OOPo</i>	71.18	0.19	1.3736	5.2516		2.2
LLS	71.63	4.70	6.1953	0.5192		2.1
<i>ALnL</i>	71.92	0.03	5.8680	0.4200	0.9741	2.1.1
OLP^a	72.79	6.40	5.8110	0.4268	0.8688	2.1.1
<i>SLnO</i>	73.30	0.30	1.3792	0.0664	0.0917	2.1.1
<i>OOM</i>	74.27	0.32	6.4804	0.6837		2.1
<i>PPoO</i>	74.27	0.39	4.1799	0.4115	0.8633	2.1.1
<i>OLG</i>	75.61	0.36	5.8878	0.3183	0.7694	2.1.1
PLP	76.21	3.09	5.4516	0.4138		2.1
<i>POM</i>	77.95	0.07	3.9525	0.2809	0.8272	2.1.1
OOO	77.92	2.30	6.3840			2
<i>BLnL^a</i>	78.51	0.06	7.0464	0.4622	1.0021	2.1.2
<i>LLA</i>	78.58	0.26	7.2240	0.5780		2.1
<i>PGL</i>	79.30	0.31	12.5441	0.3456	0.5377	2.1.1
SLO^a	80.04	3.10	6.5120	0.4423	0.9297	2.1.1
OOP	81.61	2.24	5.7333	0.6427		2.1
<i>LL-21:0</i>	82.17	0.08	5.7512	0.9080		2.1
<i>OLE^a</i>	82.87	0.07	6.4830	0.3967	0.6906	2.1.1
<i>SLP</i>	83.87	1.90	5.5518	0.3715	0.8084	2.1.1
<i>OOG</i>	84.60	0.21	4.1970	1.6582		2.2
<i>LLnLg^a</i>	85.46	0.02	7.0458	0.4700	0.9452	2.1.1
POP	85.73	0.84	5.7668	0.4204		2.1

Table 3 continued

TAG	RT (min)	Comp.	[MNH ₄] ⁺ /Σ[DAG] ⁺	[AA] ⁺ /[AB] ⁺ or [AC] ⁺ /([AB] ⁺ + [BC] ⁺)	[BC] ⁺ /[AB] ⁺	Case
<i>LBL</i>	85.81	0.40	7.2997	0.5610		2.1
<i>ALO*</i>	87.79	0.18	6.4166	0.4069	0.8337	2.1.1
<i>PGO</i>	88.84	0.17	7.1068	0.2985	0.8190	2.1.1
<i>LL-23:0</i>	89.59	0.08	6.3017	0.7648		2.1
OOS	89.70	0.87	6.9452	0.5448		2.1
<i>OL-21:0^a</i>	91.68	0.04	5.1955	0.3133	0.5113	2.1.1
<i>PPP</i>	91.83	0.01	4.4130			2
PAL	92.12	0.30	12.2610	0.2661	0.4666	2.1.1
SLS	92.15	0.56	7.4161	0.4843		2.1
OOE	92.51	0.05	2.7437	3.5188		2.2
LLLg	93.43	0.14	8.2701	0.6126		2.1
SOP	94.22	0.57	6.5034	0.3996	0.9892	2.1.1
OLB^a	95.63	0.21	7.2725	0.4265	0.9985	2.1.1
PEO	96.89	0.05	8.9111	0.4173	0.7772	2.1.1
<i>GSO</i>	96.89	0.06	12.8495	0.2385	0.4030	2.1.1
<i>LL-25:0</i>	97.19	0.03	5.8199	1.2181		2.2
OOA	97.89	0.05	7.4752	0.5660		2.1
<i>OL-23:0^a</i>	99.59	0.04	5.8422	0.3310	0.5663	2.1.1
LBP	100.18	0.20	8.1235	0.4490	0.9744	2.1.1
<i>SAL^a</i>	100.21	0.10	11.8628	0.3404	0.5194	2.1.1
<i>PPS</i>	101.14	0.01	2.5541	0.9343		2.1
<i>LLCe</i>	101.11	0.02	6.2655	0.9738		2.1
<i>OO-21:0</i>	101.93	0.01	4.1321	1.6958		2.2
<i>APO</i>	102.98	0.08	12.5880	0.2917	0.4835	2.1.1
SOS	102.98	0.15	8.4219	0.5406		2.1
<i>OLLg</i>	103.58	0.07	7.3905	0.4121	0.9389	2.1.1
OOB	105.97	0.08	7.6991	0.5772		2.1
<i>OL-25:0^a</i>	107.25	0.01	4.5772	0.2854	0.4537	2.1.1
<i>LgPL</i>	108.29	0.10	10.7037	0.3380	0.6220	2.1.1
BSL	108.31	0.08	8.6612	0.4521	0.8523	2.1.1
OO-23	109.39	0.01	4.1822	1.5642		2.2
BPO	110.26	0.05	7.8758	0.4452	1.0094	2.1.2
<i>OLCe</i>	110.38	0.02	5.8149	0.3103	0.6288	2.1.1
<i>SAO^a</i>	110.30	0.03	12.4154	0.2914	0.4251	2.1.1
OOlg	112.61	0.03	7.6458	0.6387		2.1
LSLg	114.51	0.02	7.3071	0.3851	0.7049	2.1.1
OO-25	115.29	0.00 ^b	3.8183	2.3285		2.2
OPLg	116.06	0.01	7.4666	0.4436	0.9420	2.1.1
BSO	116.46	0.01	7.9965	0.4867	0.9541	2.1.1
OOCe	117.50	0.01	7.6751	0.8731		2.1
LSCe	118.57	0.00	5.1985	0.2614	0.4378	2.1.1
OSLg	119.36	0.00	8.1439	0.4478	0.8725	2.1.1
<i>OOMo</i>	119.68	0.00	4.0893	4.3416		2.2
Sum		100.00	Avg. = 6.2732			

TAG name indicates most abundant regioisomer, as indicated by Critical Ratio 2, and order of fatty acyl chains indicated by Critical Ratio 3 set to minimum. Bold face indicates clean spectrum; italics indicate spectrum contains substantial peaks from more than one TAG. Parentheses indicate number of scans averaged, if < 15. Underlining indicates structure assigned different from APCI-MS

^a Order of FA changed after isotope correction

^b Values of 0.00 were present at less than 0.005

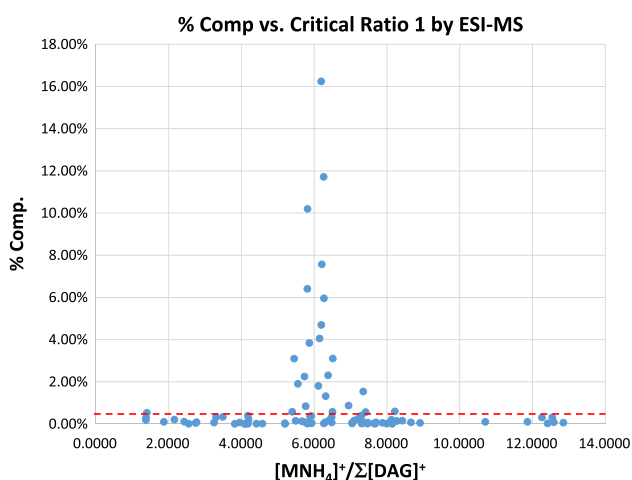


Fig. 3 Plot of percentage composition of triacylglycerols versus Critical Ratio 1, $[MNH_4]^+/\Sigma[DAG]^+$, by ESI-MS showing narrow range of values for Critical Ratio 1 for the most abundant molecular species

every TAG that was borderline to being assigned differently similarly contained $[LL]^+$ (LLS, LLA, LLLg), with LnLnP being the only TAG with a dramatically different CR2 that did not contain $[LL]^+$. Thus, CR2 by ESI-MS exhibited a distinct trend that has not been reported previously, and also pointed out the gap in knowledge regarding the need for the same kind of data for ESI-MS that Holcapek *et al.* [9] reported for APCI-MS.

By ESI-MS/MS, four TAG were also assigned as different regioisomers, with no clear universal trend apparent. ESI-MS/MS data are not discussed in detail due to space limitations, and due to the fact that auto-MS/MS did not give mass spectra for every TAG.

Critical Ratio 2 for Type III TAG

Table 1 shows that 18 Type III TAG were assigned as different regioisomers by APPI-MS (underlined in Table 1) compared to APCI-MS (not including the 5 TAG assigned differently based on Critical Ratio 3, which have the same $[1,3-DAG]^+$). These assignments were based on the observation initially reported by Mottram and Evershed [12], which indicated that the $[1,3-DAG]^+$ could be assigned based on the $[DAG]^+$ having the lowest abundance, due to the fact that loss of the FA in the *sn*-2 position was energetically disfavored. The differences in Table 1, combined with the greater influence of unsaturation on ion abundances by APPI-MS than APCI-MS exhibited by CR1, appear to indicate that the influence of unsaturation on APPI-MS is stronger than the subtle influence of loss of the FA in the *sn*-2 position. Thus, the trend reported by APCI-MS is not perfectly applicable and cannot reliably be used for assignment of the $[1,3-DAG]^+$ by

APPI-MS. This, again, is new information provided by the use of Critical Ratios for TAG structural analysis, and points again to the gap in knowledge regarding APPI-MS of structurally specific TAG regioisomers. Trends are not universally apparent, and interpretation needs to be done cautiously based on current data, due to a lack of extant APPI-MS data for comparison. Nevertheless, some trends seem to account for the majority of differences between APPI-MS and APCI-MS assignments. For instance, LnOP, LnLA, and LnLB gave the smallest fragment for Ln combined with a saturated FA. Also, PLG, OLS, PLS, PLB, OL-25:0, BLS, SLLg, and SLCE all exhibited the smallest fragment for the fully saturated or monounsaturated $[DAG]^+$ fragment, but not LO-21:0, APL, or ASL. One interesting trend that was seen in all TAG that were assigned differently by APPI-MS versus APCI-MS was that when there was a chain length mis-match for a single FA (C16, C20, C22, C24, etc. combined with two C18 FA), the mismatched FA was always part of the smallest fragment (and assigned as the $[1,3-DAG]^+$). In fact, only one TAG (i.e., OLS) of the 23 that were assigned differently was not chain mis-matched. This seems to indicate a substantial influence of chain length on APPI-MS fragment ratios, in addition to the effect of unsaturation. Clearly there is a need for additional data for regioisomers analyzed by APPI-MS in order to fully characterize their behavior. Fortunately, the Critical Ratios provide a new, useful tool for identifying trends based on the greater influence of unsaturation and chain length on APPI-MS ion abundances.

ESI-MS data in Table 3, on the other hand, gave the same structural assignments for Type III TAG as APCI-MS, apparently indicating that the same trend observed by Mottram and Evershed [12] for APCI-MS applies well to ESI-MS.

ESI-MS/MS, on the other hand, gave 11 TAG structures that were different based on CR2. Thus, ESI-MS/MS on this hyperbolic ion trap mass spectrometer cannot be used to reliably assign the $[1,3-AC]$ fragment ion without analysis of regioisomer standards on this instrument.

Critical Ratio 3 for Type III TAG

Table 1 reveals that 4 TAG (i.e., PLS, POS, OPE, POB) were assigned differently for APPI-MS versus APCI-MS based only on the assignment of the $[1,2(2,3)-AB]^+$ and $[2,3(1,2)-BC]^+$ using the Byrdwell convention [7]. Since CR3 was constructed such that $CR3 \leq 1$, so $[BC]^+ \leq [AB]^+$, the assignments made for these 4 TAG showed that the $[DAG]^+$ having the longest FA produced the smaller fragment, and was assigned as $[BC]^+$, with the shorter FA being assigned as $[AB]^+$, keeping in mind that the $[1,3-AC]^+$ was first assigned from the smallest

Table 4 Percentage of ‘ABA’ regioisomers of Type II TAG based on calibration curves from literature values [9] and observed [AA]⁺/[AB]⁺ ratios in Tables 1, 3, and Supplementary Table 1

TAG ^a	APCI-MS (%) ^b	APPI-MS (%)	ESI-MS (%)	ESI-MS/MS (%)
LnLLn	90.5	100.0	92.2	<u>45.6 %</u>
LLnL	70.5	<u>4.1</u>	<u>49.0</u>	79.4 %
LnOLn	60.7	93.7	100.0	<u>39.2 %</u>
LnLnP	0.0	6.8	49.1	0.0 %
LLM _{LLP}	0.0	0.0	0.0	0.0 %
LLO	3.2	0.0	<u>74.2</u>	0.0 %
OLnO	68.1	79.4	71.7	82.4 %
LLP	0.0	0.0	<u>59.2</u>	0.0 %
LLG _{LLO}	0.0	0.0	0.0	<u>89.6 %</u>
PLnP	100.0	100.0	100.0	100.0 %
OLO	100.0	73.1	100.0	100.0 %
MOM _{POP}	100.0	70.4	94.2	–
OOP _{OOP}	0.0	0.0	0.0	0.0 %
LLS	0.0	0.0	46.4	0.0 %
OOM _{OOP}	12.4	0.0	0.0	0.0 %
PLP	100.0	100.0	100.0	100.0 %
LLA	0.0	0.0	48.5	0.0 %
OOP	0.0	0.0	0.0	0.0 %
LL-21:0 _{LLA}	0.0	0.0	0.0	–
OOG _{OOA}	0.0	0.0	0.0	0.0 %
POP	100.0	100.0	74.9	96.7 %
LLB _{LLA}	0.0	0.0	<u>51.7</u>	0.0 %
LL-23:0 _{LLA}	0.0	0.0	12.5	–
OOS	23.1	0.0	14.2	0.9 %
SLS	60.8	100.0	74.0	<u>0.0 %</u>
OOE _{OOA}	0.0	0.0	0.0	12.9 %
LLL _{gLLA}	0.0	0.0	41.8	–
LL-25:0 _{LLA}	0.0	0.0	0.0	–
OOA	7.6	0.0	0.0	–
PPS _{PPO}	15.4	0.0	0.0	–
LLCe _{LLA}	0.0	0.0	0.0	–
OO-21:0 _{OOA}	0.0	0.0	0.0	19.6 %
SOS	100.0	95.8	57.1	87.8 %
OOB _{OOA}	19.4	0.0	0.0	15.2 %
OO-23:0 _{OOA}	0.0	0.0	0.0	0.0 %
OOL _{gOOA}	23.5	0.0	0.0	–
OO-25:0 _{OOA}	0.0	0.0	0.0	–
OOCe _{OOA}	10.5	0.0	0.0	–
OOM _{OAA}	0.0	0.0	0.0	–

^a TAG names assigned by APCI-MS^b From: Anal. Bioanal. Chem. (2015) DOI:10.1007/s00216-015-8590-9

of all [DAG]⁺ fragments. Thus, again, CR3 by APPI-MS appears to reflect a greater difference in response due to chain length than APCI-MS. Since APCI-MS data for this

Table 5 APPI-MS mass spectrum abundances calculated from critical ratios given in Table 1 processed through the Updated Bottom Up Solution

TAG	[MH] ⁺	[AA] ⁺ or [AC] ⁺	[AB] ⁺	[BC] ⁺
CyCyCy	3	100		
CyCyCa	5	55	100	
CaCaCy	5	57	100	
LnLnLn	100	8		
LnLLn	100	4	9	
LLLn	100	21	31	
LnOLn	100	4	9	
LnLM	100	5	21	8
LnLnP	100	5	6	
LLL	100	78		
LLnO	100	20	27	23
LLM	100	44	19	
LnLP	100	11	19	15
LnPPo	100	13	45	22
LnOM	100	8	42	21
LLO	100	56	62	
OLPo	68	19	100	21
OLnO	100	10	26	
LLP	100	59	63	
LOM	100	22	73	33
PoLP	79	26	100	86
LnOP	100	11	19	12
LLG	100	27	11	
PLM	26	39	100	48
PLnP	100	11	33	
OLO	100	39	79	
MOM	30	44	100	
OOPo	16	100	26	
LLS	100	29	30	
LnLA	100	7	29	8
OLP	100	48	73	53
SLnO	86	9	100	18
OOM	49	59	100	
PPoO	49	85	100	85
OLG	100	16	59	25
PLP	33	40	100	
POM	35	58	100	84
OOO	56	100		
LnLB	100	6	13	10
LLA	100	18	14	
PLG	100	13	24	16
OLS	100	31	56	37
OOP	46	58	100	
LL-21:0	100	42	14	
OLE	100	22	69	25
PLS	57	54	100	98
OOG	46	100	55	

Table 5 continued

TAG	[MH] ⁺	[AA] ⁺ or [AC] ⁺	[AB] ⁺	[BC] ⁺
LnLLg	100	6	15	8
POP	24	27	100	
LLB	100	19	16	
OLA	100	25	50	30
OPG	97	65	100	100
LL-23:0	100	30	13	
OOS	52	64	100	
LO-21:0	87	20	100	23
PPP	1	100		
APL	100	52	83	60
SLS	43	37	100	
OOE	18	100	25	
LLLg	100	20	18	
POS	43	36	100	80
OLB	100	30	56	34
OPE	95	68	100	83
GSO	100	43	75	60
LL-25:0	100	41	17	
OOA	51	74	100	
LO-23:0	100	28	87	29
PLB	71	63	100	94
ASL	100	63	89	62
PPS	6	92	100	
LLCe	100	37	19	
OO-21:0	39	100	58	
APO	100	58	83	77
SOS	35	30	100	
OLLg	100	34	73	41
OOB	46	61	100	
OL-25:0	88	32	100	34
PLLg	100	75	93	78
BLS	86	64	100	95
OO-23:0	40	100	81	
POB	58	45	100	78
OLCe	100	31	97	45
ASO	100	64	77	68
OOLg	39	63	100	
SLLg	54	48	100	83
OO-25:0	31	100	66	
POLg	47	36	100	76
BOS	27	14	64	100
OOCe	54	100	53	
SLCe	31	31	100	46
LgOS	35	53	100	94
OOMo	0	100	3	

soybean oil sample agreed well with regioisomeric assignments made by Holcapek *et al.*, we assume that the APCI-MS assignments are correct, and that the assignments made by APPI-MS are not as reliable, due to the greater effects of unsaturation and chain length on this API technique. Once again, this highlights the need for APPI-MS-specific data for synthetic regioisomers, similar to the data of Holcapek *et al.* [9] for APCI-MS.

ESI-MS data in Table 3, in contrast, gave the same structural assignments using the Byrdwell convention as were given by APCI-MS. Thus, the same trends in CR3 for APCI-MS reported by Byrdwell were reflected in the ESI-MS data.

Four Type III TAG (i.e., PoLO, GLO, ELO, OGP) in Supplementary Table 1 were reversed based on CR3 compared to APCI-MS data. However, ESI-MS/MS data will not be discussed in detail.

Application of the UBUS to APPI-MS and ESI-MS

In addition to the new trends reported above for APPI-MS and ESI-MS made possible by the Critical Ratios, the ratios in Tables 1, 3, and Supplementary Table 1 constitute compact data sets that allow the mass spectra by APPI-MS and ESI-MS to be reproduced by processing the Critical Ratios through the UBUS [7] (or the original BUS [8]). Table 5 shows the APPI-MS mass spectral abundances for the [MH]⁺ and up to three [DAG]⁺ ions. Supplementary Table 2 provides the mass spectra from ESI-MS calculated from Table 3, and Supplementary Table 3 provides the ESI-MS/MS mass spectra calculated from Supplementary Table 1.

Vitamin D₃

Vitamin D₃ quantification by APPI-MS using SIM gave results of $42.90 \pm 0.83 \mu\text{g}$ (1716 ± 33 International Units, IU) per capsule by calibration line ($r^2 = 0.9996$), and $43.02 \pm 0.87 \text{ mg}$ (1721 ± 35 IU) per capsule using the RF approach, in good agreement to the corresponding values reported by APCI-MS of 1759 ± 74 IU and 1722 ± 71 IU by IS and RF approaches, respectively. These results indicate that the results by APPI-MS were statistically indistinguishable from SIM results by APCI-MS for these samples. Although results from EICs gave similar results, 1720 ± 154 IU and 1663 ± 147 IU for IS and RF approaches, respectively, the use of EICs for quantification is not recommended, due to the better S/N in SIM chromatograms and the lower standard deviations in results by SIM.

Conclusion

The Critical Ratios constitute a reduced data set because it takes fewer values to express the Critical Ratios (one Critical Ratio for Type I TAG, two Critical Ratios for Type II TAG, and three Critical Ratios for Type III TAG) than it takes to express the raw abundances (two abundances, the $[MH]^+$ and one $[DAG]^+$, for Type I TAG, three for Type II TAG, and four for Type III). Furthermore, the Critical Ratios provide more information at face value than the raw abundances. For instance, CR2 is used to quantify regioisomers, not raw abundances. Thus, the Critical Ratios actually provide *more information in fewer values* than the raw abundances.

Most importantly, the Critical Ratios make subtle trends more apparent, allow never-before defined trends to be elucidated, even after two decades of TAG analysis by APCI-MS, and even longer by ESI-MS. Commercially available APPI-MS is a relatively more recent development, and the Critical Ratios can be seen from the data above to allow trends to be seen that have not yet been reported. For instance, the greater effect of the degree of unsaturation and carbon chain length are important factors that must be taken into consideration as use of this API technique matures over the coming years. The Critical Ratios and the UBUS constitute very useful tools that allow TAG to be more fully characterized than some other approaches that have been reported.

Acknowledgments The work of Dr. Robert Goldschmidt to conduct fatty acid methyl ester analysis by GC-FID is gratefully acknowledged. This work was supported by the USDA Agricultural Research Service. Mention or use of specific products or brands do not represent or imply endorsement by the USDA.

Compliance with Ethical Standards

Conflict of interest The author declares that he has no conflict of interest.

References

- Hunter JE (2001) Studies on effects of dietary fatty acids as related to their position on triglycerides. *Lipids* 36(7):655–668
- Karupaiah T, Sundram K (2007) Effects of stereospecific positioning of fatty acids in triacylglycerol structures in native and randomized fats: a review of their nutritional implications. *Nutr Metab*. doi:10.1186/1743-7075-4-16
- Dubois V, Breton S, Linder M, Fanni J, Parmentier M (2007) Fatty acid profiles of 80 vegetable oils with regard to their nutritional potential. *Eur J Lipid Sci Technol* 109(7):710–732. doi:10.1002/ejlt.200700040
- Schwab U, Lauritzen L, Tholstrup T, Haldorsson T, Riserus U, Uusitupa M, Becker W (2014) Effect of the amount and type of dietary fat on cardiometabolic risk factors and risk of developing type 2 diabetes, cardiovascular diseases, and cancer: a systematic review. *Food Nutr Res*. doi:10.3402/fnr.v58.25145
- Chowdhury R, Warnakula S, Kunutsor S, Crowe F, Ward HA, Johnson L, Franco OH, Butterworth AS, Forouhi NG, Thompson SG, Khaw KT, Mozaffarian D, Danesh J, Di Angelantonio E (2014) Association of dietary, circulating, and supplement fatty acids with coronary risk: a systematic review and meta-analysis. *Ann Intern Med* 160(6):398–406
- Scientists fix errors in controversial paper about saturated fats (2014) <http://news.sciencemag.org/health/2014/03/scientists-fix-errors-controversial-paper-about-saturated-fats>. Accessed 25 Mar 2014
- Byrdwell WC (2015) The Updated Bottom Up Solution applied to mass spectrometry of soybean oil in a dietary supplement gelcap. *Anal Bioanal Chem* 407(17):5143–5160. doi:10.1007/s00216-015-8590-9
- Byrdwell WC (2005) The Bottom Up Solution to the triacylglycerol lipidome using atmospheric pressure chemical ionization mass spectrometry. *Lipids* 40(4):383–417. doi:10.1007/s11745-006-1398-9
- Holcapek M, Dvorakova H, Lisa M, Giron AJ, Sandra P, Cvacka J (2010) Regioisomeric analysis of triacylglycerols using silver-ion liquid chromatography-atmospheric pressure chemical ionization mass spectrometry: comparison of five different mass analyzers. *J Chromatogr A* 1217(52):8186–8194
- Jakab A, Jablonkai I, Forgács E (2003) Quantification of the ratio of positional isomer dilinoleoyl-oleoyl glycerols in vegetable oils. *Rapid Commun Mass Spectrom* 17(20):2295–2302
- Byrdwell WC (2005) Qualitative and quantitative analysis of triacylglycerols by atmospheric pressure ionization (APCI and ESI) mass spectrometry techniques. In: Byrdwell WC (ed) *Modern methods for lipid analysis by liquid chromatography/mass spectrometry and related techniques*. AOCS Press, Champaign, pp 298–412
- Mottram HR, Evershed RP (1996) Structure analysis of triacylglycerol positional isomers using atmospheric pressure chemical ionisation mass spectrometry. *Tetrahedron Lett* 37(47):8593–8596
- Laakso P, Voutilainen P (1996) Analysis of triacylglycerols by silver-ion high-performance liquid chromatography-atmospheric pressure chemical ionization mass spectrometry. *Lipids* 31(12):1311–1322
- Byrdwell WC, Emken EA (1995) Analysis of triglycerides using atmospheric pressure chemical ionization mass spectrometry. *Lipids* 30(2):173–175. doi:10.1007/BF02538272
- Iwasaki Y, Yasui M, Ishikawa T, Irimescu R, Hata K, Yamane T (2001) Optical resolution of asymmetric triacylglycerols by chiral-phase high-performance liquid chromatography. *J Chromatogr A* 905(1–2):111–118. doi:10.1016/S0021-9673(00)00989-4
- Lisa M, Holcapek M (2013) Characterization of triacylglycerol enantiomers using chiral HPLC/APCI-MS and synthesis of enantiomeric triacylglycerols. *Anal Chem* 85(3):1852–1859. doi:10.1021/ac303237a
- Řezanka T, Kolouchová I, Čejková A, Cajthaml T, Sigler K (2013) Identification of regioisomers and enantiomers of triacylglycerols in different yeasts using reversed- and chiral-phase LC-MS. *J Sep Sci* 36(20):3310–3320. doi:10.1002/jssc.201300657
- Řezanka T, Sigler K (2014) Separation of enantiomeric triacylglycerols by chiral-phase HPLC. *Lipids* 49(12):1251–1260. doi:10.1007/s11745-014-3959-7
- Byrdwell WC (2011) “Dilute-and-shoot” triple parallel mass spectrometry method for analysis of vitamin D and triacylglycerols in dietary supplements. *Anal Bioanal Chem* 401(10):3317–3334. doi:10.1007/s00216-011-5406-4

20. Byrdwell WC, Neff WE, List GR (2001) Triacylglycerol analysis of potential margarine base stocks by high-performance liquid chromatography with atmospheric pressure chemical ionization mass spectrometry and flame ionization detection. *J Agric Food Chem* 49(1):446–457. doi:[10.1021/jf0008801](https://doi.org/10.1021/jf0008801)
21. Byrdwell WC, Emken EA, Neff WE, Adlof RO (1996) Quantitative analysis of triglycerides using atmospheric pressure chemical ionization-mass spectrometry. *Lipids* 31(9):919–935
22. Byrdwell WC (2013) Quadruple parallel mass spectrometry for analysis of vitamin D and triacylglycerols in a dietary supplement. *J Chromatogr A* 1320:48–65. doi:[10.1016/j.chroma.2013.10.031](https://doi.org/10.1016/j.chroma.2013.10.031)
23. Byrdwell WC (2014) Extract-filter-shoot liquid chromatography with mass spectrometry for the analysis of vitamin D₂ in a powdered supplement capsule and standard reference material 3280. *J Sep Sci* 37(16):2095–2110. doi:[10.1002/jssc.201400234](https://doi.org/10.1002/jssc.201400234)
24. Patiny L, Borel A (2013) ChemCalc: a building block for tomorrow's chemical infrastructure. *J Chem Inf Model* 53(5):1223–1228. doi:[10.1021/ci300563h](https://doi.org/10.1021/ci300563h)
25. Yamamoto H, McCloskey JA (1977) Calculations of isotopic distribution in molecules extensively labeled with heavy isotopes. *Anal Chem* 49(2):281–283
26. Byrdwell WC, Neff WE (2002) Dual parallel electrospray ionization and atmospheric pressure chemical ionization mass spectrometry (MS), MS/MS and MS/MS/MS for the analysis of triacylglycerols and triacylglycerol oxidation products. *Rapid Commun Mass Spectrom* 16(4):300–319. doi:[10.1002/rcm.581](https://doi.org/10.1002/rcm.581)